Duality between equilibrium and nonequilibrium networks

Dmitri Krioukov[1] and Massimo Ostilli[1,2]

[1] *Cooperative Association for Internet Data Analysis, University of California San Diego, CA, USA*
[2] *Statistical Mechanics and Complexity Center (SMC), INFM-CNR SMC, Rome, Italy*

In statistical physics any given system can be either at an equilibrium or away from it. Networks are not an exception. Most network models can be safely classified as either equilibrium or growing. Here we show that if certain conditions are satisfied, there exists a growing counterpart for any equilibrium network model, and vice versa. The equivalence between the two systems is exact not only asymptotically, but even for any finite system size. The required conditions are satisfied in causal sets and to a large extent in some real complex networks.

PACS numbers: 89.75.Hc, 89.75.Fb, 05.40.-a, 04.20.Gz

Statistical physics studies equilibrium and nonequilibrium systems using different theory and methods, as these systems are drastically different. Networks are not an exception. The vast realm of network models can be roughly divided into equilibrium and nonequilibrium domains [1, 2]. In the former, one usually builds an equilibrium ensemble of graphs of a given size. Classic examples are classical random graphs [3], soft configuration model and hidden variable models [4], or random geometric graphs [5]. In nonequilibrium models, graphs usually grow by adding nodes one at a time, introducing statistical dependencies. Preferential attachment [6, 7] is perhaps the best known example. These two approaches are clearly different [4, 8, 9]. In the simplest example, i.e. classical random graphs $\mathcal{G}_{N,p}$, each pair of N nodes are independently connected with the same probability p. The resulting degree distribution is Poissonian with mean $\bar{k} = pN$. In a growing version of this model, new nodes $N = 1, 2, 3, \ldots$ are coming one at a time connecting to each existing nodes with probability $p = \bar{k}/N$. The degree distribution is exponential [1].

Causal sets (or causets) [10] can, on the one hand, be considered as random geometric graphs in Lorentzian spaces: distribute nodes uniformly at random, using a Poisson point process, over (a compact patch of) a Lorentzian manifold, and then connect each node pair located at timelike distance [10]. This construction is clearly equilibrium. On the other hand, causets were proposed as a model of quantum gravity, in which case they must be a dynamic model of growing spacetime [11]. To approximate the spacetime that we observe, this currently unknown dynamics, if run to completion (thermodynamic or large-size limit), must lead to asymptotically the same graphs as in the static case, reminiscent of the connection between Cayley trees and Bethe lattices [12]. This imperative duality between stasis and dynamics is somewhat unusual in physics. It raises many questions, including philosophical [13], while the causet quantum gravity program is far from complete.

Notwithstanding these difficulties, causets in asymptotically de Sitter spacetimes [14], such as the spacetime of our accelerating universe [15, 16], are structurally similar to real complex networks, e.g. the brain or Internet [17]. This similarity is a consequence of asymptotic equivalence between the growth dynamics of de Sitter causets and complex networks [17]. Specifically, a growing model of complex networks [18] is asymptotically identical to growing de Sitter causets [17], leading to an apparent paradox: given that only an equilibrium construction for de Sitter causets is currently known, what are these "growing causets," or more generally, how can a graph model be equilibrium and nonequilibrium at the same time?

Here we show that if certain conditions are satisfied, then there exists a dynamic (growing) counterpart $\mathcal{G}_D$ for any static (equilibrium) graph model $\mathcal{G}_S$, and vice versa. Specifically we prove that $\mathcal{G}_S$ and $\mathcal{G}_D$ are identical, and that this equivalence is exact not only asymptotically, but even for any finite graph size. That is, if $\mathcal{G}_S$ generates graph G with probability $P(G)$, then so does $\mathcal{G}_D$. For concreteness we work with de Sitter causets in $1+1$ dimensions, and generalize at the end.

Static $1+1$-dimensional de Sitter causets can be defined as follows [17]. Given volume V and sprinkling density δ as parameters defining the expected size $\bar{N} = \delta V$ and average degree of resulting graphs:

1) sample graph size N from the Poisson distribution

$$\mathbb{P}_{\delta V}(N) = e^{-\delta V}\frac{(\delta V)^N}{N!}; \qquad (1)$$

2) sample N random numbers v_i, $i = 1, \ldots, N$, from the uniform distribution on $[0, V]$, shorthand $v_i \in \mathcal{U}(0, V)$;

3) assign to each node i its conformal time and space coordinates given by $\eta_i = \arctan[v_i/(2\pi)]$ and $\theta_i \in \mathcal{U}(0, 2\pi)$;

4) connect each pair of nodes i and j if $\Delta\eta > \Delta\theta$, where $\Delta\eta = |\eta_i - \eta_j|$ and $\Delta\theta = \pi - |\pi - |\theta_i - \theta_j||$ are the temporal and spatial distances between the two nodes.

The first two steps in this definition are nothing but an implementation of a Poisson point process (PPP) with rate δ on $[0, V]$. The third step is a PPP on a compact patch $\mathcal{V}$ of volume V in de Sitter spacetime between conformal times $\eta = 0$ and $\eta_0 = \arctan[V/(2\pi)]$. The element of volume in this spacetime is $dV = \sec^2\eta\, d\eta\, d\theta$, and step (3) ensures that the spatial and temporal node

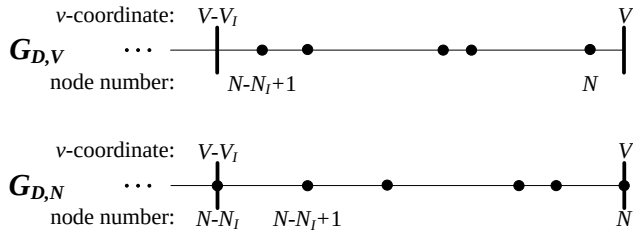

FIG. 1: Illustration of the Poisson point process in $\mathcal{G}_{D,V}$ (top) and $\mathcal{G}_{D,N}$ (bottom).

densities are $\rho(\theta) = 1/(2\pi)$ and $\rho(\eta) = \sec^2\eta/\tan\eta_0$, meaning that nodes are indeed distribution uniformly at random in $\mathcal{V}$ according to the volume form dV. The resulting graphs have a power-law distribution of node degrees k, $P(k) \sim k^{-\gamma}$, with $\gamma = 2$, and strongest possible clustering [17]. We denote this ensemble by $\mathcal{G}_{S,V}$.

We now want to build a dynamic version of this ensemble, $\mathcal{G}_{D,V}$, by adding nodes one at a time. Unfortunately it is impossible if we want $\mathcal{G}_{D,V}$ to be identical to $\mathcal{G}_{S,V}$. The best we can do is the following $\mathcal{G}_{D,V}$ definition. For $I = 1, 2, \ldots$:

1) select any real number $V_I \geq 0$ and let $V = \sum_{J=1}^{I} V_J$;

2) sample $N_I \in \mathbb{P}_{\delta V_I}(N_I)$ and let $N = \sum_{J=1}^{I} N_J$;

3) for $i = N - N_I + 1, \ldots, N$, sample $v_i \in \mathcal{U}(V - V_I, V)$ and $\theta_i \in \mathcal{U}(0, 2\pi)$, and set $\eta_i = \arctan[v_i/(2\pi)]$;

4) connect all new nodes $i = N - N_I + 1, \ldots, N$ to all existing nodes $j = 1, \ldots, N$ if $\Delta\eta > \Delta\theta$.

Each time I we simply grow the spacetime patch $\mathcal{V}$ that nodes occupy, by adding to $\mathcal{V}$ a new spacetime chunk $\mathcal{V}_I$ of volume V_I, and throwing N_I new nodes into $\mathcal{V}_I$, Fig. 1(top). If all $V_I = 1/\delta$, then the expected number of nodes we add each time is $\bar{N}_I = 1$. However, we cannot force the number of new nodes N_I to be exactly 1. Indeed, suppose we freeze the $\mathcal{G}_{D,V}$ growing process at some volume V, and compare the result to the static $\mathcal{G}_{S,V}$ construction. If we have been adding exactly one node in each $\mathcal{V}_I$, then the number of nodes $N_I = 1$ in $\mathcal{V}_I$ is clearly different from what it is in $\mathcal{G}_{S,V}$, where this number can be anything—by the PPP definition, it is Poisson-distributed around 1. Step (2) in the $\mathcal{G}_{D,V}$ definition ensures that the N_I distributions are the same in both cases. The expected numbers of nodes $\bar{N}$ in generated graphs G are also the same, for any partition of $\mathcal{V}$ in $\mathcal{G}_{S,V}$ into chunks $\{\mathcal{V}_I\}$ in $\mathcal{G}_{D,V}$, because a sum of Poisson-distributed random numbers is Poisson-distributed with the mean equal to the sum of means.

Probability $P(G)$ to generate any graph G is the same in $\mathcal{G}_{S,V}$ and $\mathcal{G}_{D,V}$, i.e. the two ensembles are identical, if the linking conditions for node pairs are the same, which is clearly the case here ($\Delta\eta > \Delta\theta$), and if the distributions of node coordinates (η, θ) are exactly the same, too. The latter does hold as a simple consequence of the PPP definition, i.e. of the fact the expected number of nodes in any volume element dV is $dN = \delta\, dV$. For example, let N be the number of nodes in a $\mathcal{G}_{S,V}$ sample. Then in the v-coordinates, the expected number of nodes lying between v and $v + dv$ in the sample is $N\rho(v)\, dv$, where $\rho(v) = 1/V$ is the PDF of v-coordinates. The expected number of nodes in $[v, v + dv]$ in the static ensemble is then

$$dN_S(v) = \sum_{N=0}^{\infty} N\rho(v)\mathbb{P}_{\delta V}(N)\, dv = \delta\, dv. \qquad (2)$$

Assume now $v \in \mathcal{V}_I$ for some I in $\mathcal{G}_{D,V}$, where the v-PDF is $\rho_I(v) = 1/V_I$. The same number in the dynamic ensemble is then

$$dN_D(v) = \sum_{N_I=0}^{\infty} N_I\rho_I(v)\mathbb{P}_{\delta V_I}(N_I)\, dv = \delta\, dv, \qquad (3)$$

i.e. $dN_D(v) = dN_S(v)$. As a consequence, in the η-coordinates, the expected number of nodes in an infinitesimal spacetime chunk between η and $\eta + d\eta$ is in both cases

$$dN(\eta) = \delta\, dV(\eta) = 2\pi\delta\sec^2\eta\, d\eta, \qquad (4)$$

so that the probability density functions (PDFs) for η are indeed the same, Fig. 2(a,b), and equal to

$$\rho(\eta) = \frac{dN(\eta)}{N\, d\eta} = \frac{\sec^2\eta}{\tan\eta_0}. \qquad (5)$$

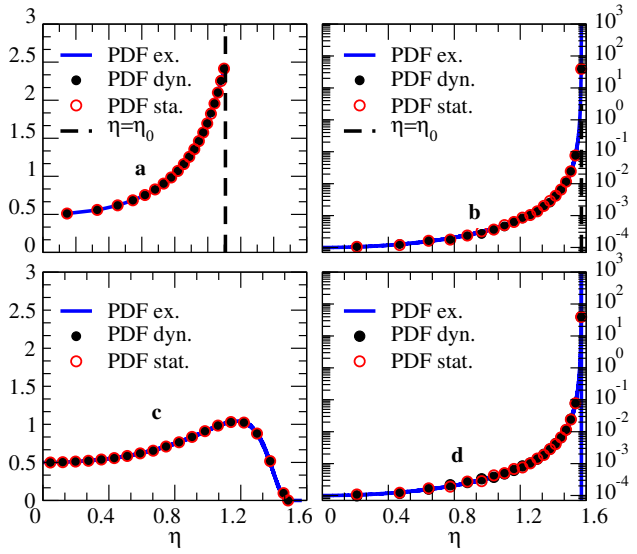

FIG. 2: Probability density functions (PDFs) for conformal time coordinates η in static and dynamic ensembles. Panels (a) and (b) deal with the fixed-V ensembles $\mathcal{G}_{S,V}$ and $\mathcal{G}_{D,V}$, where the exact η-PDF is given by Eq. (5), the solid blue curves. The red circles and black dots are simulation results for $\mathcal{G}_{S,V}$ and $\mathcal{G}_{D,V}$. In (a), $V = 2 \times 2\pi$, $I = 2$, $V_1 = V_2 = 2\pi$, and $\eta_0 = 1.107148$. In (b), $V = 2\pi \times 10^4$, $I = 10^4$, $V_1 = \ldots = V_{10^4} = 2\pi$, and $\eta_0 = 1.570696$. Panels (c) and (d) show the corresponding results for fixed-N ensembles $\mathcal{G}_{S,N}$ and $\mathcal{G}_{D,N}$, where the exact PDF is given by Eq. (9). In (c), $N = 2$, $I = 2$, $N_1 = N_2 = 1$. In (d), $N = 10^4$, $I = 10^4$, $N_1 = \ldots = N_{10^4} = 1$. The numbers of samples (PPP runs) in simulations are $S = 10^6$ in (a) and (c), and $S = 10^4$ in (b) and (d). The sprinkling density (PPP rate) is $\delta = 1$ everywhere.

The equivalence between the coordinate one-point PDFs $\rho(\eta)$ is a necessary but not sufficient condition for two ensembles to be the same. The sufficient condition is that the joint distributions $\rho(\eta_1, \eta_2, \ldots)$ are also the same. If they are different, then even if their marginals $\rho(\eta)$ are the same, some other graph properties can be different, even in the thermodynamic limit. One example would be the order statistics [19] defining, among other things, the distribution of the smallest time coordinate $\eta_{\min}$ of nodes, and consequently the distributions of their largest $k_{\max}$ and average $\bar{k}$ degrees. The joint coordinate distributions in $\mathcal{G}_{S,V}$ and $\mathcal{G}_{D,V}$ are the same, also as a PPP consequence. Both ensembles implement the same PPP process, so that due to statistical independence of PPP events (nodes), the joint PDFs are products of one-point PDFs in both cases. In other words, the two ensembles are indeed exactly the same, and generate any graph G with the same probability $P(G)$.

But is it really impossible to add exactly one, or to that end, any fixed number of nodes at a time, as in many popular models of growing networks, including preferential attachment? The answer is that it is certainly possible, but the resulting ensembles $\mathcal{G}_{S,N}$ and $\mathcal{G}_{D,N}$ that we define next are identical to $\mathcal{G}_{S,V}$ and $\mathcal{G}_{D,V}$ only in the thermodynamic limit. Yet in a certain sense that becomes evident from the exposition below, $\mathcal{G}_{S,N}$ and $\mathcal{G}_{D,N}$ are dual to $\mathcal{G}_{S,V}$ and $\mathcal{G}_{D,V}$ for any finite graph size.

We first define the static ensemble $\mathcal{G}_{S,N}$ of graphs of a fixed size N, dual to $\mathcal{G}_{S,V}$. Given graph size N and sprinkling density δ as parameters defining the expected spacetime volume $\bar{V} = N/\delta$ occupied by nodes, and the average degree in resulting graphs:

1) sample spacetime volume V from the Gamma distribution

$$\Gamma_{N,\delta}(V) = e^{-\delta V} \frac{(\delta V)^N}{N!} \frac{N}{V} \tag{6}$$

dual to the Poisson distribution, and set $v_N = V$;

2) sample $N-1$ random numbers $v_i \in \mathcal{U}(0, V)$, $i = 1, \ldots, N-1$;

3) assign to each node $i = 1, \ldots, N$ its conformal time and space coordinates given by $\eta_i = \arctan[v_i/(2\pi)]$ and $\theta_i \in \mathcal{U}(0, 2\pi)$;

4) connect each pair of nodes i and j if $\Delta\eta > \Delta\theta$.

Since the Gamma distribution $\Gamma_{N,\delta}(V)$ is the distribution of waiting time V for the N'th outcome of a PPP with rate δ, the $\mathcal{G}_{S,N}$ definition implements the same PPP as $\mathcal{G}_{S,V}$, except that not the waiting time V but the number of events N is now fixed.

The dynamic variant $\mathcal{G}_{D,N}$ is now obvious. For $I = 1, 2, \ldots$:

1) select any integer number $N_I \geq 0$ and let $N = \sum_{J=1}^{I} N_J$;

2) sample $V_I \in \Gamma_{N_I,\delta}(V_I)$, let $V = \sum_{J=1}^{I} V_J$, and set $v_N = V$;

3) for $i = N - N_I + 1, \ldots, N-1$, sample $v_i \in \mathcal{U}(V - V_I, V)$, and for $i = N - N_I + 1, \ldots, N$ sample $\theta_i \in \mathcal{U}(0, 2\pi)$ and set $\eta_i = \arctan[v_i/(2\pi)]$;

4) connect all new nodes $i = N - N_I + 1, \ldots, N$ to all existing nodes $j = 1, \ldots, N$ if $\Delta\eta > \Delta\theta$.

As in the fixed-V case, we add nodes in bunches, except that the number of new nodes that we add each time is now fixed, see Fig. 1(bottom). In particular this number can be always 1. Yet we cannot strictly control the volume that these nodes occupy, as we could not control the number of nodes in the volume-controlled case $\mathcal{G}_{*,V}$.

The $\mathcal{G}_{S,N}$ and $\mathcal{G}_{D,N}$ ensembles are identical for any partition $\{N_I\}$ of any N, since the two ensembles are two different implementations of the same fixed-N PPP. In particular, the expected volume $\bar{V}$ that nodes occupy is the same in both cases because the sum of Gamma-distributed random variables is Gamma-distributed with the mean equal to the sum of means. The expected number of nodes in any volume element dV is $dN = \delta\, dV$ as before, but the one-point PDFs for time coordinates are different from $\mathcal{G}_{*,V}$, where the v- and η-PDFs are defined on finite intervals $[0, V]$ and $[0, \eta_0]$ with $\eta_0 < \pi/2$, while in $\mathcal{G}_{*,N}$ even at $N = 1$ the single node can have an arbitrarily large coordinate, meaning that the corresponding distributions are defined on the whole infinite space $[0, \infty)$ and $[0, \pi/2)$. For example, since the distribution of the v-coordinate of i'th node in the PPP is given by $\rho_i(v) = \Gamma_{i,\delta}(v)$, the PDF of v-coordinates for N nodes is simply

$$\rho(v) = \frac{1}{N} \sum_{i=1}^{N} \Gamma_{i,\delta}(v) = \frac{\delta}{N} Q(N, \delta v), \text{ where} \tag{7}$$

$$Q(N, \delta v) = \frac{\Gamma(N, \delta v)}{\Gamma(N)} \tag{8}$$

is the regularized Gamma function. The η-PDF is then

$$\rho(\eta) = \frac{\delta}{N} \sec^2 \eta\; Q(N, \delta \tan \eta), \tag{9}$$

see Fig. 2(c,d).

It is instructive to consider the following ensemble $\mathcal{G}_{W,N}$ where 'W' stands for "wrong": for $i = 1, \ldots, N$, sample $v_i \in \Gamma_{i,\delta}(v_i)$, and then finish the graph construction as before. The intuition might be that since i'th coordinate is distributed according to $\Gamma_{i,\delta}(v)$, we can safely sample directly from this distribution, and one can check that if we do so, then the v-PDF is as needed, $\rho(v) = (\delta/N) Q(N, \delta v)$. However, this reasoning is wrong. The process is no longer a PPP, and the joint PDFs are different from $\mathcal{G}_{S,N}$ and $\mathcal{G}_{D,N}$, because the ordering of coordinates can now be violated, e.g. v_i can with certain probability be larger than v_j for any $i < j$, while by definition, $\Gamma_{i,\delta}(v)$ is the distribution of the i'th largest coordinate in a PPP. As a result $\mathcal{G}_{W,N}$ is not identical to $\mathcal{G}_{S,N}$ and $\mathcal{G}_{D,N}$ even in the thermodynamic limit, which one can verify in simulations by looking at the maximum and average degree statistics, for instance.

In the thermodynamic limit $N \to \infty$, the regularized Gamma function approaches 1, $Q(N, \delta v) \to 1$, so that $\rho(v) \to \delta/N$ and $\rho(\eta) \to (\delta/N) \sec^2 \eta$, and the fixed-$N$

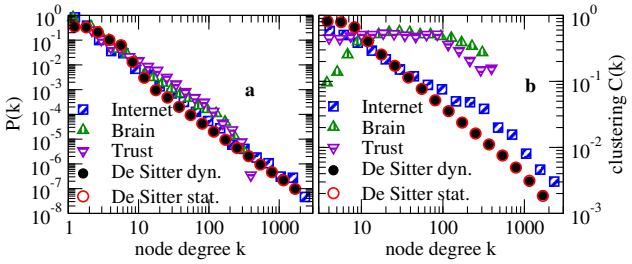

FIG. 3: Degree distribution (a) and clustering (b) in de Sitter causets $\mathcal{G}_{S,N}$ and $\mathcal{G}_{D,N}$, 1000 samples each of size $N = 23752$, sprinkling density $\delta = 0.834751/2\pi$, average degree $\bar{k} = 4.9188$ and average clustering $\bar{c} = 0.7862$ and $\bar{c} = 0.7854$, respectively, and in some real networks: AS Internet ($N = 23752$, $\bar{k} = 4.9188$, $\bar{c} = 0.6055$), functional brain network ($N = 23713$, $\bar{k} = 6.1436$, $\bar{c} = 0.1552$), and PGP Web of Trust ($N = 23797$, $\bar{k} = 7.8587$, $\bar{c} = 0.4816$).

ensembles $\mathcal{G}_{S,N}$ and $\mathcal{G}_{D,N}$ become asymptotically identical to the fixed-V ensembles $\mathcal{G}_{S,V}$ and $\mathcal{G}_{D,V}$, all implementing the same PPP on the infinite upper half of de Sitter spacetime with $\eta > 0$. In other words, we have proved the following diagram

$$\begin{array}{ccc} \mathcal{G}_{S,V} & = & \mathcal{G}_{D,V} \\ \wr & & \wr \\ \mathcal{G}_{S,N} & = & \mathcal{G}_{D,N} \end{array}$$

where the equal sign '=' means the exact equivalence for any system size, while symbol '$\sim$' stands for asymptotic equivalence and for the V.vs.N PPP duality at finite sizes.

In general, the same picture would apply to any pair of static and dynamic network models in which the joint distributions of (hidden or latent) variables [4], attributes, or coordinates of nodes, including their birth times, are the same, and in which the probabilities of connections between nodes, as functions of these hidden variables, are exactly the same, too. Surprisingly, these two conditions are rarely satisfied. As a result, static and evolving networks are analyzed using quite different methods. To the best of our knowledge, there is no equilibrium construction that would be exactly identical to preferential attachment, for instance. Yet the required conditions are satisfied in causal sets and more generally, in random geometric graphs, including random geometric graphs in hyperbolic spaces [18]. These hyperbolic graphs are asymptotically identical to de Sitter causets [17], and describe well not only the structure but also the dynamics of some real networks [18]. Here we have to stress that this hyperbolic-de Sitter equivalence is exact only for a specific (default) set of parameters [18], leading to specific types of graphs—namely, to graphs with power-law exponent $\gamma = 2$, and with strongest possible clustering, i.e. zero temperature [18]. The former property applies to many real networks, Fig. 3(a), but the latter does not, explaining differences between clustering in de Sitter causets and real networks, Fig. 3(b). However, the temperature of real networks is low, meaning that their clustering, while not the strongest possible, is still strong and thermodynamically stable [18]. In that respect the differences between de Sitter causets and real networks may be not that big.

In conclusion, almost all real networks are growing, justifying certain concerns, if not skepticism, about the utility of equilibrium methods in analyzing real networks. Yet the structure and dynamics of these networks turn out to be well described by network models characterized by the unusual exact equivalence between equilibrium and nonequilibrium formulations that we have proved here. These results thus provide a different perspective and further theoretical grounds for the use of powerful equilibrium methods, including exponential random graphs and other graph entropy tools [20–29], in the analysis of real networks.

Acknowledgments

We thank D. Meyer, D. Rideout, S. Dorogovtsev, P. Krapivsky, and Z. Toroczkai for useful discussions and suggestions. This work was supported by DARPA grant No. HR0011-12-1-0012; NSF grants No. CNS-0964236 and CNS-1039646; and by Cisco Systems.

[1] S. N. Dorogovtsev and J. F. F. Mendes, *Evolution of Networks: From Biological Nets to the Internet and WWW* (Oxford University Press, Oxford, 2003).
[2] M. E. J. Newman, *Networks: An Introduction* (Oxford University Press, Oxford, 2010).
[3] R. Solomonoff and A. Rapoport, B Math Biophys **13**, 107 (1951).
[4] M. Boguñá and R. Pastor-Satorras, Phys Rev E **68**, 36112 (2003).
[5] M. Penrose, *Random Geometric Graphs* (Oxford University Press, Oxford, 2003).
[6] P. L. Krapivsky, S. Redner, and F. Leyvraz, Phys Rev Lett **85**, 4629 (2000).
[7] S. N. Dorogovtsev, J. F. F. Mendes, and A. N. Samukhin, Phys Rev Lett **85**, 4633 (2000).
[8] P. Bialas, Z. Burda, J. Jurkiewicz, and A. Krzywicki, Phys Rev E **67**, 66106 (2003).
[9] P. Bialas, Z. Burda, and B. Waclaw, AIP Conf Proc **776**, 14 (2005).
[10] L. Bombelli, J. Lee, D. Meyer, and R. Sorkin, Phys Rev Lett **59**, 521 (1987).
[11] D. Rideout and R. Sorkin, Phys Rev D **61**, 024002 (1999).
[12] M. Ostilli, Physica A **391**, 3417 (2012).
[13] C. Wüthrich, J Gen Philos Sci (2013), URL `http://dx.doi.org/10.1007/s10838-012-9205-1`.
[14] S. W. Hawking and G. F. R. Ellis, *The Large Scale Struc-*

ture of Space-Time (Cambridge University Press, Cambridge, 1975).
[15] S. Perlmutter, G. Aldering, M. D. Valle, S. Deustua, R. S. Ellis, S. Fabbro, A. Fruchter, G. Goldhaber, D. E. Groom, I. M. Hook, et al., Nature **391**, 51 (1998).
[16] A. G. Riess, A. V. Filippenko, P. Challis, A. Clocchiatti, A. Diercks, P. M. Garnavich, R. L. Gilliland, C. J. Hogan, S. Jha, R. P. Kirshner, et al., Astron J **116**, 1009 (1998).
[17] D. Krioukov, M. Kitsak, R. S. Sinkovits, D. Rideout, D. Meyer, and M. Boguñá, Sci Rep **2**, 793 (2012).
[18] F. Papadopoulos, M. Kitsak, M. A. Serrano, M. Boguñá, and D. Krioukov, Nature **489**, 537 (2012).
[19] H. David and H. Nagaraja, *Order Statistics* (Wiley-Interscience, New York, 2003).
[20] J. Park and M. E. J. Newman, Phys Rev E **70**, 66117 (2004).
[21] D. Garlaschelli and M. Loffredo, Phys Rev Lett **102**, 38701 (2009).
[22] T. Squartini and D. Garlaschelli, New J Phys **13**, 083001 (2011).
[23] G. Bianconi, Europhys Lett **81**, 28005 (2008).
[24] G. Bianconi, P. Pin, and M. Marsili, Proc Natl Acad Sci USA **106**, 11433 (2009).
[25] K. Anand and G. Bianconi, Phys Rev E **80**, 045102(R) (2009).
[26] K. Anand, G. Bianconi, and S. Severini, Phys Rev E **83**, 036109 (2011).
[27] K. Zhao, A. Halu, S. Severini, and G. Bianconi, Phys Rev E **84**, 066113 (2011).
[28] K. Zhao, M. Karsai, and G. Bianconi, PloS One **6**, e28116 (2011).
[29] J. West, G. Bianconi, S. Severini, and A. E. Teschendorff, Sci Rep **2**, 802 (2012).